[DOI]10.12016/j.issn.2096-1456.2021.11.002

· 基础研究 ·

钛表面微弧氧化–微波水热法铜铌涂层的制备及抗菌性研究

王天琦[1]，　杜青[2]，　谢伟丽[1]
1.哈尔滨医科大学口腔医学院修复科，黑龙江 哈尔滨(150001)；　2.哈尔滨工业大学材料科学与工程学院，黑龙江 哈尔滨(150001)

【摘要】 **目的**　在钛表面通过微弧氧化-微波水热两步法制备铜铌抗菌涂层，对其表面结构和抗菌性能进行探究。**方法**　以包覆微弧氧化涂层(MAO组)的钛为基体，通过微波水热法分别在低(MHL-Cu组)、中(MHM-Cu组)、高(MHH-Cu组)浓度的氯化铜溶液及草酸铌(MH-Nb组)溶液中引入铜、铌元素。通过能谱分析确定引入铜最多的组分，与草酸铌混合微波水热制备铜铌复合涂层(MH-Cu/Nb组)。通过扫描电子显微镜、X射线能谱仪及X射线衍射仪对各组试件微观结构、元素分布和物相成分进行表征；贴膜法测定涂层对大肠杆菌和金黄色葡萄球菌的抑菌效果。**结果**　X射线能谱仪显示MHL-Cu、MHM-Cu、MHH-Cu组表面均引入了Cu元素，各组铜元素原子比例依次为(0.68 ± 0.04)%、(1.17 ± 0.06)%、(1.64 ± 0.03)%，组间差异有统计学意义(P < 0.01)。扫描电子显微镜显示MAO组表面呈火山口状多孔结构，MHL-Cu、MHM-Cu、MHH-Cu、MH-Nb、MH-Cu/Nb组均保持微孔形貌，随Cu^{2+}浓度增加，粗糙度增加；其中MH-Nb、MH-Cu/Nb组同时出现沟壑状结构。X射线衍射仪显示MAO组涂层主要由钛和锐钛矿相TiO_2组成，MHL-Cu、MHM-Cu、MHH-Cu、MH-Nb、MH-Cu/Nb组涂层主要由锐钛矿和金红石相TiO_2组成。与MAO组菌落相比，MHH-Cu、MH-Nb、MH-Cu/Nb组大肠杆菌和金黄色葡萄球菌均有不同程度减少，差异具有统计学意义(P < 0.001)；MHH-Cu组与MH-Cu/Nb组相比，菌落数差异无统计学意义(P > 0.05)。**结论**　微弧氧化-微波水热两步法制备的含铜铌粗糙多孔的涂层可有效抑制大肠杆菌和金黄色葡萄球菌生长。

【关键词】 钛；　涂层；　表面处理；　微弧氧化；　微波水热；　铜；　铌；　抗菌；　大肠杆菌；　金黄色葡萄球菌

开放科学(资源服务)标识码(OSID)

【中图分类号】 R78　【文献标志码】 A　【文章编号】 2096-1456(2021)11-0733-07

【引用著录格式】 王天琦，杜青，谢伟丽. 钛表面微弧氧化–微波水热法铜铌涂层的制备及抗菌性研究[J]. 口腔疾病防治, 2021, 29(11): 733-739. doi: 10.12016/j.issn.2096-1456.2021.11.002.

Preparation and antibacterial properties of a copper-niobium coating on a titanium surface by a microarc oxidation-microwave hydrothermal method

WANG Tianqi[1], DU Qing[2], XIE Weili[1]. 1. Department of Prosthodontics, College of Stomatology, Harbin Medical University, Harbin 150001, China; 2. School of Materials Science and Engineering, Harbin Institute of Technology, Harbin 150001, China
Corresponding author: XIE Weili, Email: xwl811@126.com, Tel: 86-451-85553231

【Abstract】 **Objective**　To prepare a copper-nobium antibacterial coating on a titanium surface by a microarc oxidation-microwave hydrothermal two-step method and to study its surface structure and antibacterial properties. **Methods** Using titanium coated with a microarc oxidation coating (MAO group) as the substrate, copper and niobium were introduced by a microwave hydrothermal method in low (MHL-Cu group), medium (MHM-Cu group) and high (MHH-Cu group) copper chloride solutions and niobium oxalate (MH-Nb group) solutions, respectively. The component with the highest copper content was determined by energy spectrum analysis, and the copper-niobium composite coating (MH-Cu/

【收稿日期】2021-03-04；【修回日期】2021-04-28
【基金项目】黑龙江省科技攻关项目(GC12C305-3)
【作者简介】王天琦，医师，硕士，Email：349530444@qq.com
【通信作者】谢伟丽，主任医师，博士，Email：xwl811@126.com，Tel：86-451-85553231

Nb group) was prepared by microwave hydrothermal mixing with niobium oxalate. The microstructure, element distribution and phase composition of the specimens were characterized by scanning electron microscopy, energy dispersive spectrometry and X-ray diffraction, and the bacteriostatic effect of the coating on *Escherichia coli* and *Staphylococcus aureus* was determined by the film method. **Results** Energy dispersive spectrometry showed that Cu was introduced onto the surface of the MHL-Cu, MHM-Cu, and MHH-Cu groups, and the atomic ratios of copper in each group were (0.68 ± 0.04)%, (1.17 ± 0.06)%, and (1.64 ± 0.03)%. The difference between groups was statistically significant (P < 0.01). Scanning electron microscopy showed a crater-like porous structure on the surface of the MAO group, and the MHL-Cu, MHM-Cu, MHH-Cu, MH-Nb, MH-Cu/Nb groups maintained micropore morphology. The roughness increased with increasing Cu^{2+} concentration, in which the MH-Nb and MH-Cu/Nb groups showed gully like structures simultaneously. X-ray diffraction showed that the coating of the MAO group was mainly composed of titanium and anatase phase TiO_2, and the coatings of the MHL-Cu, MHM-Cu, MHH-Cu, MH-Nb, MH-Cu/Nb groups were mainly composed of anatase and rutile phase TiO_2. Compared with the MAO group, *Escherichia coli* and *Staphylococcus aureus* in the MHH-Cu, MH-Nb, MH-Cu/Nb groups decreased to varying degrees, with significant differences (P < 0.001); compared with the MH-Cu/Nb group, the colony number difference had statistical significance (P > 0.05). **Conclusion** The rough, porous coating containing copper and niobium prepared by the microarc oxidation-microwave hydrothermal two-step method can effectively inhibit the growth of *Escherichia coli* and *Staphylococcus aureus*.

【Key words】 titanium; coating; surface treatment; microarc oxidation; microwave hydrothermal; copper; niobium; antibacterial; *Escherichia coli; Staphylococcus aureus*

J Prev Treat Stomatol Dis, 2021, 29(11): 733-739.

【Competing interests】 The authors declare no competing interests.

This study was supported by Science and Technology Key Projects of Heilongjiang Province (No. GC12C305-3).

钛及钛合金由于优异的机械性能、高耐腐蚀性及良好的生物相容性等，被广泛应用于骨科手术及牙科种植体[1]。植入物表面改性是减少植入物相关感染发生的有效途径，同时也是可以在不破坏材料本身性能的情况下改性植入物界面属性相对简单的方法[2]。微弧氧化技术虽然可以通过调控电解液成分引入到涂层中一些生物活性元素，但部分生物活性元素以非晶形式存在于涂层内不具备好的生物活性，微波水热处理能更好地赋予涂层生物活性及活化表面性能[3]。铜离子在一定浓度下具有抗菌性能和生物活性，且不会对细菌产生耐药性[4]。铌具有较高的化学稳定性和生物相容性，含有铌元素的磷酸钙复合涂层可显著增加成骨细胞的碱性磷酸酶活性，具有促进成骨细胞钙化的作用[5]，但目前对于含铌涂层抗菌性能相关文献较少。本实验拟采用微弧氧化法在纯钛表面制备含钙磷元素陶瓷涂层，通过微波水热法合成含铜铌的涂层，观察分析涂层的结构表征，并测定其抗菌效果。

1　材料与方法

1.1　实验材料及菌株

纯钛TA2（江浙钛制品有限公司，中国）；大肠杆菌（*Escherichia coli*，*E. coli*）国际标准菌株（ATCC25922）与金黄色葡萄球菌（*Staphylococcus aureus*，*S. aureus*）国际标准菌株（ATCC29213）均由哈尔滨兽医研究所提供。

1.2　实验试剂及主要仪器设备

LB培养基（luria-bertni culture，LB culture）（百思生物技术有限公司，中国）；氯化铜（天津福晨化学试剂公司，中国）；草酸铌（上海麦克林生化科技有限公司，中国）；微弧氧化设备（MAO60-Ⅱ，西安理工大学，中国）；微波水热平行合成仪（XH-800S；北京祥鹄科技发展有限公司，中国）；扫描电子显微镜（scanning electron microscope，SEM）（Helios Nanolab 600i，FEI，美国）；X射线能谱仪（energy dispersive spectrometer，EDS）（Helios Nanolab 600i，EDAX，美国）；常温/高温多功能X射线衍射仪（X-ray diffraction，XRD）（X'PERT，Panalytical，荷兰）；生化培养箱（KB115，Binder，德国）。

1.3　实验方法

1.3.1　试件的制备及分组　将纯钛TA2用线切割加工成标准试件10 mm × 10 mm × 1 mm，表面预处理，依次用240#、400#、800#、1 000#的SiC砂纸打磨去除其表面氧化层。将试件浸没在丙酮、无水乙醇、去离子水超声清洗30 min，吹干备用。

① MAO组：预处理后的钛试件为阳极，不锈钢

为阴极，置于带有搅拌系统的电解液中，将MAO60-Ⅱ型脉冲电源升至预设电压，制备MAO涂层。电解液成分如表1所示。工艺参数见表2。

表1 微弧氧化电解液成分

Table 1 Composition of the microarc oxidation electrolyte

The name of reagent	Content(g/L or mL/L)	Purity
EDTA-2Na	15.0	>99%
$Ca(CH_3COO)_2·H_2O$	8.8	>98%
$Ca(H_2PO_4)_2·H_2O$	6.3	>98%
$Na_2SiO_3·9H_2O$	7.1	>98%
NaOH	5.0	>98%
H_2O_2	6.0	30%

表2 微弧氧化工艺参数

Table 2 Process parameters of the microarc oxidation

Control mode	Voltage (V)	Time (min)	Duty cycle (%)	Frequency (Hz)
Constant voltage mode	400	5	8	600

②MH-Cu组：将带有MAO涂层的钛片用夹具将其固定在微波水热反应釜中，样品完全浸没在40 mL不同浓度的$CuCl_2$溶液中，放入XH-800S型微波水热平行合成仪中。微波水热处理引入Cu^{2+}工艺参数及分组如表3。反应完成后，待样品自然冷却至室温后取出。去离子水冲洗，烘干备用。

表3 不同浓度$CuCl_2$溶液微波水热处理的分组及工艺参数

Table 3 Grouping and process parameters of microwave hydrothermal treatment of $CuCl_2$ solutions with different concentrations

Experiment groups	$CuCl_2$ concentration (mol/L)	Temperature (℃)	Holding time (min)
MHL-Cu	0.1	200	60
MHM-Cu	0.5	200	60
MHH-Cu	1.0	200	60

③MH-Nb组：纯钛试件微弧氧化处理后，以0.1 mol/L的草酸铌为反应液微波水热法制备含铌涂层，处理方法同MH-Cu组。

④MH-Cu/Nb组：根据扫描电子显微镜和能谱仪选择MH-Cu组中引入铜最多的组别与0.1 mol/L的草酸铌溶液混合微波水热制备铜铌涂层，处理方法同MH-Cu组。

1.3.2 涂层表面形貌、元素分析、物相组成 SEM下对涂层微观结构进行观察；EDS测定涂层表面元素种类、含量及其元素面分布；XRD对表面物相组成进行分析。

1.3.3 贴膜法测定抗菌性能 LB培养基分别接种冻干株*E. coli*和*S. aureus*，37 ℃恒温培养24 h后，再将其传至两代，接种环取菌株在LB液体培养基中，37 ℃恒温培养24 h，最后用麦氏比浊法将菌悬液浓度稀释至1×10^6 CFU/mL。贴膜法测定本实验中MAO组、MH-Cu组中Cu^{2+}引入量最多组、MH-Nb组、MH-Cu/Nb组表面涂层，将20 μL菌悬液滴在24孔板上的样品表面，用无菌性的PE薄膜(0.855 cm × 0.85 cm)覆盖，在菌液均匀分布、不溢出状态下37 ℃培养24 h。将试样取出后置于20 mL的PBS中洗脱5 min。将100 μL洗脱液滴在LB固体培养基上，37 ℃恒温培养24 h后菌落平板计数。抗菌率=[(对照组平均回收菌落数-实验组平均回收菌落数)/对照组平均回收菌落数]×100%。

1.4 统计学分析

采用SPSS 23.0软件对实验数据进行统计，数据符合正态性和方差齐性，以$\bar{x} \pm s$表示，多组间比较采用单因素方差分析，两两比较采用LSD检验分析，$P < 0.05$为差异有统计学意义。

2 结 果

2.1 表面元素含量、分布分析

EDS显示，MHL-Cu、MHM-Cu、MHH-Cu组表面均引入了Cu元素，各组Cu元素原子比例依次为(0.68 ± 0.04)%、(1.17 ± 0.06)%、(1.64 ± 0.03)%，差异有统计学意义($P < 0.01$)，因而选择MHH-Cu组与草酸铌混合经微波水热制备复合涂层(MH-Cu/Nb组)。图1为MHH-Cu组涂层表面元素扫描图，可以看出各元素分布均匀，Ti元素分布较为广泛，在微孔处含量较多；O、Si、P、Ca、Cu元素主要分布在微孔周围，在孔内含量较少。图2、图3分别为MH-Nb、MH-Cu/Nb组表面元素分布图，与引入Cu元素类似，各元素分布均匀，Ti含量较多，分布在微孔处，其他元素主要分布在孔洞周围。

2.2 涂层表面形貌分析

图4a为MAO组的SEM图，呈现典型的“火山口状”形貌，孔洞分布均匀，孔隙率为8.83%，通过右上角高倍扫描图可以观察到涂层表面较为光滑。MH-Cu组表面形貌如图4b ~ 4d所示，涂层表面仍保持着多孔结构，随着Cu^{2+}浓度的增加，孔洞尺寸变化不大，孔隙率略有下降(依次为8.13%、7.39%、6.92%)，粗糙度增加，颗粒物粒径变大。MH-Nb组涂层表面仍保持着火山状微孔(图4e)，

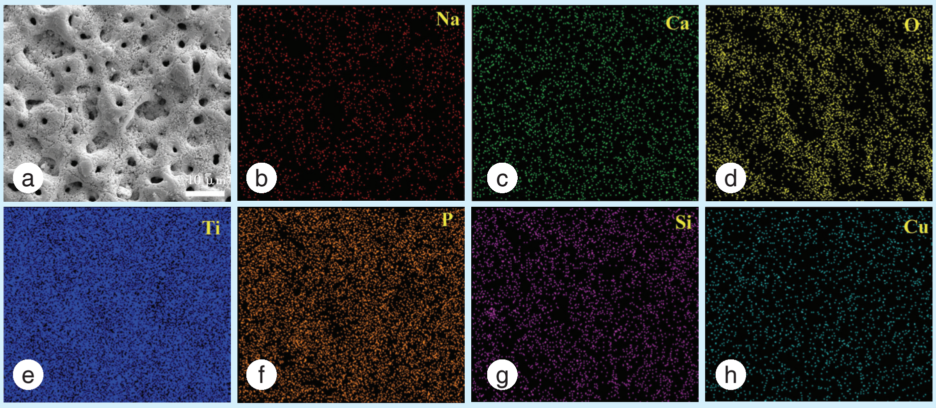

a: SEM morphology of the MHH-Cu group, 1 mol/LCuCl$_2$ solution microwave hydrothermal treatment coating; b: Na elements uniformly distributed around the micropores; c: Ca elements uniformly distributed around the micropores; d: O elements uniformly distributed around the micropores; e: Ti elements widely distributed and more micropores; f: P elements uniformly distributed around the micropores; g: Si elements uniformly distributed around the micropores; h: Cu elements uniformly distributed around the micropores

Figure 1　Distribution of elements on the surface of a microwave hydrothermal coating with a high copper content (× 5 000)

图 1　高铜组微波水热涂层表面元素分布(× 5 000)

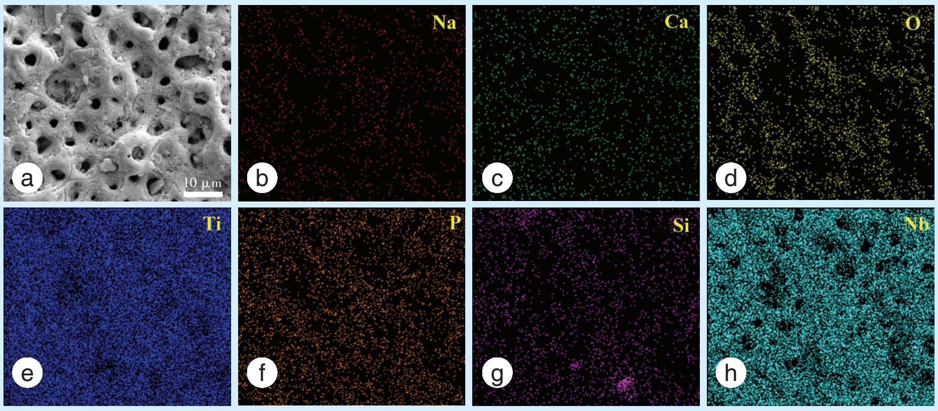

a: SEM morphology of the MH-Nb group, 1 mol/L $C_{10}H_5NbO_{20}$ solution microwave hydrothermal treatment coating; b: Na elements uniformly distributed around the micropores; c: Ca elements uniformly distributed around the micropores; d: O elements uniformly distributed around the micropores; e: Ti elements widely distributed and more micropores; f: P elements uniformly distributed around the micropores; g: Si elements uniformly distributed around the micropores; h: Nb elements uniformly distributed around the micropores

Figure 2　Distribution of the elements on the surface of the microwave hydrothermal coating containing niobium (× 5 000)

图 2　含铌组微波水热涂层表面元素分布(× 5 000)

孔隙率(9.26%)较 MAO 涂层有所增加,表面出现沟壑状,颗粒物较小,局部存在大颗粒沉积。MH-Cu/Nb 组涂层表面微孔尺寸变化不大(图 4f),但孔隙率达到 11.2%,涂层表面沟壑状明显,沉积物较多。

2.3　表面物相分析

MAO 组主要是 Ti 和锐钛矿(Anatase)TiO_2的衍射峰,含有少量的金红石(Rutile)相,TiO_2的存在与能谱中元素含量相吻合(图 5)。实验组可同时观测到 Anatase 和 Rutile 相 TiO_2的衍射峰,Rutile 相 TiO_2的衍射峰较 MAO 组有所增强。各组的 Anatase 和 Rutile 相 TiO_2的衍射峰强度基本相同。

2.4　贴膜法抗菌性能分析

贴膜法测定各组试件表面培养 24 h 对 *E. coli* 和 *S. aureus* 生长情况的影响(图 6),菌落计数见表 4。*E. coli* 和 *S. aureus* 的菌落数分别为 MAO 组:(590.3 ± 23.0)CFU、(488.0 ± 21.0)CFU,MHH-Cu 组:(46.0

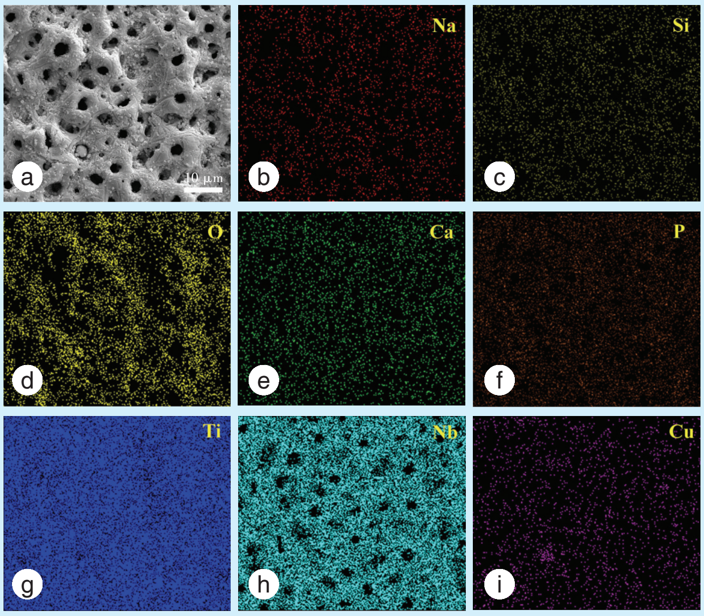

a: SEM morphology of the MH-Cu/Nb group, 1 mol/L $CuCl_2$ solution and 1 mol/L $C_{10}H_5NbO_{20}$ solution microwave hydrothermal treatment coating; b: Na elements uniformly distributed around the micropores; c: Si elements uniformly distributed around the micropores; d: O elements uniformly distributed around the micropores; e: Ca elements uniformly distributed around the micropores; f: P elements uniformly distributed around the micropores; g: Ti elements widely distributed and more micropores; h: Nb elements uniformly distributed around the micropores; i: Cu elements uniformly distributed around the micropores

Figure 3　Distribution of elements on the surface of the microwave hydrothermal coating of the copper-niobium composite group (× 5 000)

图 3　铜铌复合组微波水热涂层表面元素分布（× 5 000）

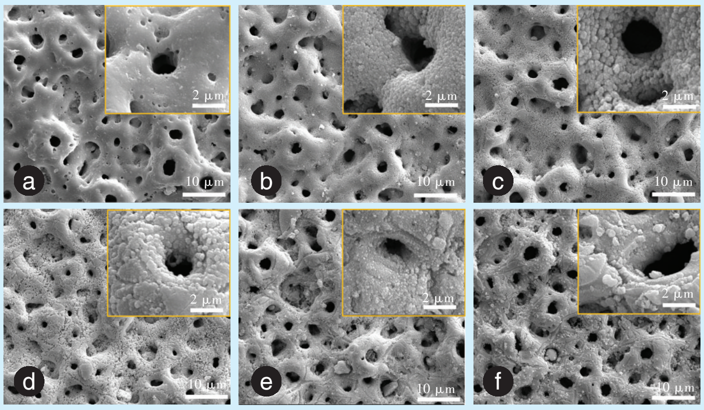

a: MAO group, crater-like morphology, smooth surface; b: MHL-Cu group, porous structure, small grain-like substance with rough surface; c: MHM-Gu group, porous structure, rough surface granular substance; d: MHH-Cu group, porous structure, rough surface with larger particles; e: MH-Nb group, porous and ravine-like structure, rough surface with deposits; f: MH-Cu/Nb group, porous and obvious ravine-like structure, with more rough surface deposits

Figure 4　Surface scanning electron microscope morphology of the coatings on each group of specimens

图 4　各组试件涂层的表面扫描电子显微镜形貌

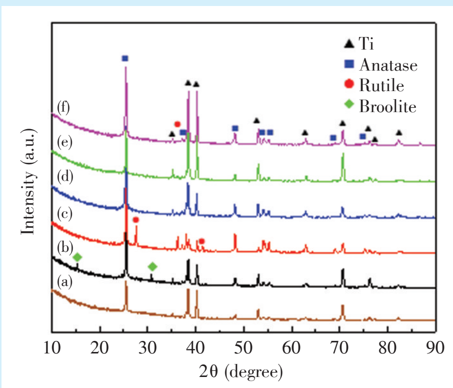

(a): MAO group, the coating consists mainly of Ti and Anatase TiO_2; (b): MHL-Cu group, the coating consists of Ti、Anatase and Rutile TiO_2, and a little Brookite TiO_2; (c): MHM-Cu group, the coating consists of Ti、Anatase and Rutile TiO_2; (d): MHH-Cu group, the coating consists of Ti、Anatase and Rutile TiO_2; (e): MH-Nb group, the coating consists of Ti、Anatase and Rutile TiO_2; (f): MH-Cu/Nb group, the coating consists of Ti、Anatase and Rutile TiO_2

Figure 5　X-ray diffraction patters of the different groups

图 5　各组 X 射线衍射仪图谱

± 5.7）CFU、（34.7 ± 3.5）CFU，MH-Nb 组：（273.0 ± 9.2）CFU、（213.0 ± 7.0）CFU，MH-Cu/Nb 组：（39.0 ± 2.6）CFU、（28.3 ± 2.1）CFU，与 MAO 组相比，MHH-Cu、MH-Nb、MH-Cu/Nb 组 *E. coli* 和 *S. aureus* 菌落数均有不同程度减少，差异具有统计学（$P < 0.001$）；MHH-Cu、MH-Cu/Nb 组 *E. coli* 和 *S. aureus* 菌落数均少于

MH-Nb组，差异具有统计学意义（P < 0.001）；MHH-Cu组*E. coli*和*S. aureus*菌落数与MH-Cu/Nb组相比，差异无统计学意义（P = 0.521，P = 0.510），但两者对*E. coli*和*S. aureus*的抗菌率均达到92%以上。

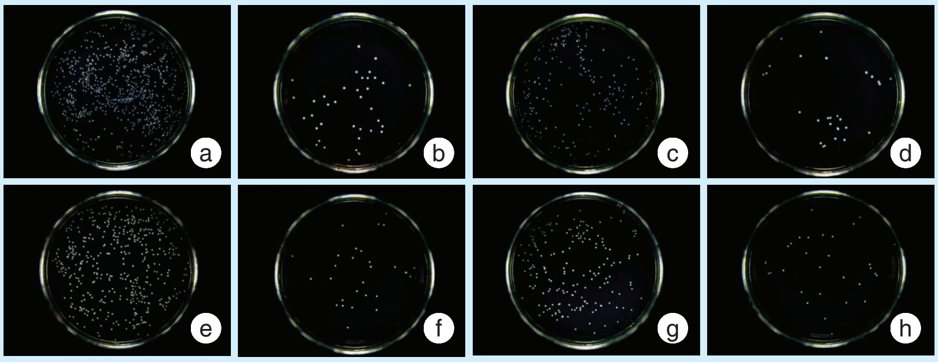

a: MAO group, *Escherichia coli* grew in large numbers and densely, with a small amount of fusion; b: MHH-Cu group, the number of *Escherichia coli* was significantly reduced and isolated; c: MH-Nb group,the number of *Escherichia coli* was reduced and loose; d: MH-Cu/Nb group, the number of *Escherichia coli* was significantly reduced and isolated; e: MAO group, *Staphylococcus aureus* grew in large numbers and densely; f: MHH-Cu group, the number of *Staphylococcus aureus* was significantly reduced and isolated; g: MH-Nb group, reduced number of *Staphylococcus aureus* and loose growth; h: MH-Cu/Nb group, the number of *Staphylococcus aureus* decreased significantly and grew in isolation

Figure 6　*Escherichia coli* and *Staphylococcus aureus* after 24 h surface culture of each group of specimens

图6　各组试件表面培养24 h后大肠杆菌和金黄色葡萄球菌的情况

表4　各组试件对大肠杆菌和金黄色葡萄球菌的抗菌效果

Table 4　Antibacterial effect of each group on *Escherichia coli* and *Staphylococcus aureus*　n=3, $\bar{x} \pm s$

Groups	*Escherichia coli*		*Staphylococcus aureus*	
	Colony count（CFU）	Antibacterial rate（%）	Colony count（CFU）	Antibacterial rate（%）
MAO	590.3±23.0	-	488.0±21.0	-
MHH-Cu	46.0±5.7[1)]	92.2	34.7±3.5[1)]	92.9
MH-Nb	273.0±9.2[1)2)]	53.8	213.0±7.0[1)2)]	56.4
MH-Cu/Nb	39.0±2.6[1)3)]	94.4	28.3±2.1[1)3)]	94.2
F	1 237.560		1 102.054	
P	< 0.001		< 0.001	

1): compared with MAO group, P < 0.001; 2): compapred with MHH-Cu group, P < 0.001; 3): compared with MH-Nb group, P < 0.001

3　讨　论

影响植入物周围软硬组织的种植体周围炎是牙种植最常见的并发症之一[6]，在种植体表面粘附的细菌被认为是生物膜形成的初始和关键步骤，这会导致种植体的失败。因此，对生物材料表面改性获得抗菌材料涂层以抑制病原微生物的粘附是目前研究的重点[7]。Scarano等[8]认为细菌一旦早期定植，可能构成一个细菌库，随后可能污染种植体的周围环境，并干扰种植体周围软硬组织的健康，进一步影响骨整合。

微弧氧化是以轻金属为阳极，不锈钢板为阴极，首先在基体表面形成阳极氧化绝缘层，随着电压升高，绝缘层被击穿，金属基体在弧光放电产生的高温高压的作用下发生氧化，形成多孔纳米结构的陶瓷涂层[9]。本实验中，微弧氧化后形成了多孔的表面涂层，这种多孔结构可以促进周围新的骨组织向内生长和血管的生成，且结合牢固[10]。微波水热是在高温、高压、微波的共同作用下，提高反应物的活性，能快速有效将生物活性元素引入涂层中，同时保留生物活性元素的优势[11]。SEM结果显示，同MAO组相较，微波水热处理的涂层表面仍保持了微弧氧化独特的多孔结构，同时MH-Cu组随着铜离子浓度增加，涂层表面孔隙率减小，粗糙度增加，颗粒物粒径稍有增加，MH-Nb、MH-Cu/Nb组涂层孔隙率与MAO组相比略有增加，这可能是草酸铌微波水热过程中释放气体引起的，颗粒物粒径较小，局部有沉积物。

羟基磷灰石主要由磷酸钙组成，是骨组织的主要成分，磷酸钙的形成在种植体与周围的骨组织之间产生了强烈的化学键，可以改善骨组织和种植体材料的同化[12]。本研究发现，经过微波水热方法，成功地在MAO涂层表面引入了相应的抗菌元素。同时，钙、磷等元素仍保持在涂层表面，说明微波水热过程不会破坏涂层诱导HA的能

力。经过不同溶液微波水热处理后的涂层，各组涂层均以Anatase和Rutile相TiO_2矿物成分组成，没有检测到含Cu或者Nb的相，可能是由于Cu、Nb含量较少或以非晶形式掺杂在MAO层表面。而Anatase和Rutile TiO_2能够诱导HA形成，促进成骨细胞增殖分化[13]。涂层表面粗糙多孔结构及钙磷等活性元素对于成骨方面作用已有大量研究，本实验主要研究如何提高该涂层的抗菌性能。

Cu作为人体必需的微量元素，有研究表明将Cu离子作为抗菌离子引入钛及钛合金中时对大肠杆菌和金黄色葡萄球菌有着明显的抑菌效果[14]。而含Nb的涂层会增加种植体抗腐蚀性及生物相容性[15]。Wojcieszak等[16]利用高能磁控溅射制备含有Cu和Nb的二氧化钛的涂层，与未掺杂的TiO_2涂层相比，TiO_2(Nb，Cu)的粗糙度较高，同时具有很好的抗菌性能。同样本实验中抗菌结果显示，与MAO组相比，MHH-Cu、MH-Nb、MH-Cu/Nb组均具有抑菌效果，而MHH-Cu组与MH-Cu/Nb组，对大肠杆菌和金黄色葡萄球菌的抗菌率均达到92%以上，效果显著，这可能与Cu离子的释放相关。

综上所述，使用微弧氧化-微波水热两步法对纯钛表面改性，成功制备了含铜、铌、钙、磷等活性元素的粗糙多孔涂层，有效抑制大肠杆菌和金黄色葡萄球菌生长。然而铜铌涂层的抗菌机制及对于其他优势菌属的抗菌性能还需进一步研究。

【Author contributions】 Wang TQ performed the experiments and wrote the article. Du Q and Xie WL designed the study. All authors read and approved the final manuscript as submitted.

参考文献

[1] Ottria L, Lauritano D, Andreasi Bassi M, et al. Mechanical, chemical and biological aspects of titanium and titanium alloys in implant dentistry[J]. J Biol Regul Homeost Agents, 2018, 32(2 Suppl. 1): 81-90.

[2] Chouirfa H, Bouloussa H, Migonney V, et al. Review of titanium surface modification techniques and coatings for antibacterial applications[J]. Acta Biomater, 2019, 83: 37-54. doi: 10.1016/j.actbio.2018.10.036.

[3] Zhao QM, Yang HL, Liu ZT, et al. Fabrication of hydroxyapatite on pure titanium by micro-arc oxidation coupled with microwave-hydrothermal treatment[J]. J Mater Sci Mater Med, 2015, 26(2): 88. doi: 10.1007/s10856-015-5429-z.

[4] Zhuang Y, Ren L, Zhang S, et al. Antibacterial effect of a copper-containing titanium alloy against implant-associated infection induced by methicillin-resistant *Staphylococcus aureus*[J]. Acta Biomater, 2021, 119: 472-484. doi: 10.1016/j.actbio.2020.10.026.

[5] Tamai M, Isama K, Nakaoka R, et al. Synthesis of a novel beta-tricalcium phosphate/hydroxyapatite biphasic calcium phosphate containing niobium ions and evaluation of its osteogenic properties [J]. J Artif Organs, 2007, 10(1): 22-28. doi: 10.1007/s10047-006-0363-y.

[6] Zhao YC, Cao HL, Qin H, et al. Balancing the osteogenic and antibacterial properties of titanium by codoping of Mg and Ag: an *in vitro* and *in vivo* study[J]. Acs Applied Materials & Interfaces, 2015, 7(32): 17862-17836. doi: 10.1021/acsami.5b04168.

[7] 周雯, 彭显, 程磊. 口腔种植体表面影响细菌黏附因素的研究进展[J]. 口腔疾病防治, 2020, 28(2): 102-106. doi: 10.12016/j.issn.2096-1456.2020.02.008.
Zhou W, Peng X, Cheng L. Research progress on factors affecting bacterial adhesion on the oral implant surface[J]. J Prev Treat Stomatol Dis, 2020, 28(2): 102 - 106. doi: 10.12016/j.issn.2096 - 1456.2020.02.008.

[8] Scarano A, Valbonetti L, Degidi M, et al. Implant-abutment contact surfaces and microgap measurements of different implant connections under 3 - Dimensional X - Ray microtomography[J]. Implant Dent, 2016, 25(5): 656 - 662. doi: 10.1097/id.0000000000000465.

[9] Pan X, Li Y, Abdullah AO, et al. Micro/nano-hierarchical structured TiO_2 coating on titanium by micro-arc oxidation enhances osteoblast adhesion and differentiation[J]. Royal Society Open Science, 2019, 6(4): 182031. doi: 10.1098/rsos.182031.

[10] Insua A, Monje A, Wang HL et al. Basis of bone metabolism around dental implants during osseointegration and peri-implant bone loss[J]. J Biomed Mater Res A, 2017, 105(7): 2075-2089. doi: 10.1002/jbm.a.36060.

[11] Yu W, Sun TW, Ding Z, et al. Copper-doped mesoporous hydroxyapatite microspheres synthesized by a microwave-hydrothermal method using creatine phosphate as an organic phosphorus source: application in drug delivery and enhanced bone regeneration[J]. J Mater Chem B, 2017, 5(5): 1039-1052. doi: 10.1039/c6tb02747d.

[12] Kulkarni Aranya A, Pushalkar S, Zhao M, et al. Antibacterial and bioactive coatings on titanium implant surfaces[J]. J Biomed Mater Res A, 2017, 105(8): 2218-2227. doi: 10.1002/jbm.a.36081.

[13] Ran W, Tian ZH, Guo B, et al. Superior biocompatibility and osteogenic efficacy of micro-arc oxidation-treated titanium implants in the canine mandible[J]. Biomed Mater, 2009, 4(5): 055003. doi: 10.1088/1748-6041/4/5/055003.

[14] Ghosh R, Swart O, Westgate S, et al. Antibacterial copper-hydroxyapatite composite coatings via electrochemical synthesis[J]. Langmuir, 2019, 35(17): 5957-5966. doi: 10.1021/acs.langmuir.9b00919.

[15] Li Y, Munir KS, Lin J, et al. Titanium-niobium pentoxide composites for biomedical applications[J]. Bioact Mater, 2016, 1(2): 127-131. doi: 10.1016/j.bioactmat.2016.10.001.

[16] Wojcieszak D, Kaczmarek D, Adamiak B, et al. Influence of Cu and Nb additives on specific surface properties and biological activity of transparent TiO_2 thin-film coatings[J]. Polim Med, 2013, 43(3): 141-146.

（编辑　罗燕鸿，曾曙光）

官网　　公众号